CREEP – FATIGUE INTERACTION AND LIFE TIME PREDICTION OF AISI 316 STAINLESS STEEL AT 550°C

M. MARCHIONNI, D. RANUCCI
CNR – ITM Via Induno 10, 20092 Cinisello B. (Milano), Italy

ABSTRACT

The AISI 316 austenitic stainless steel has been tested at 550°C in air with different strain rates, R ratio and with a hold time superimposed. During each test the presence of a strong hardening effect is generally observed, more marked at low strain rates and at high strain levels. The fatigue life is sensibly reduced at very low strain rates and in presence of a hold time. The Coffin–Manson relationship adequately describes the fatigue life in the different experimental testing conditions. The Ostergren relationship is less accurate and presents a large scatter.

KEYWORDS

Stainless steel, low cycle fatigue, strain rate, hold time, life prediction models.

INTRODUCTION

The AISI 316 austenitic stainless steel has found wide application in numerous engineering components which require good mechanical properties and corrosion resistance at temperatures up to 650°C. The 316 version with a nitrogen content of 0.08% for improving the precipitation hardening was selected for nuclear application, as fast breeder reactors, in which material stability and good fatigue resistance to cyclic loads are required. The start–up and stop–down during service conditions induce different thermomechanical cycles in the components, that are subjected to creep, fatigue and creep – fatigue interaction.
The AISI 316 has been widely studied to evaluate creep (Lai, 1979, Shinya, 1986, Yagi, 1988, Piques, 1989), fatigue (Halford, 1973, Marchionni, 1984, Brinkman, 1985, Korn, 1989) and stability (Weiss, 1972, Hanninen, 1989, Miyabara, 1995) properties, but few data are available for testing in the regime of creep – fatigue interaction (Manfredi, 1982, Pineau, 1989).
In the present work the fatigue behaviour of the alloy at 550°C is studied and the influence of the creep – fatigue interaction is evaluated by changing strain rate and by

introducing hold time in tension. The results are analysed by Coffin–Manson and Ostergren relationships modified for frequency effects in order to predict fatigue life even in presence of creep – fatigue interaction.

MATERIAL AND EXPERIMENTAL TECHNIQUES

The AISI 316 austenitic stainless steel used in this investigation was supplied in the form of 50 mm thick plate after solution treatment (1060°C/ 55 minutes/ water quenched). The chemical composition is given in Table 1. Figure 1 shows the metallographic aspect which evidences an average grain size of 90 μm (≅ 4 ASTM).

LCF tests were performed on cylindrical specimens machined from the plate. The minimum diameter was 8.5 mm and the gauge length was 25 mm. The specimens were heated at the temperature of 550°C by a three zones resistance furnace. Tests were carried out in longitudinal strain controlled conditions with a triangular wave form and a zero mean value (R= –1). The strain rates used were as follows: $10^{-2}\cdot s^{-1}$, $10^{-3}\cdot s^{-1}$, $5\cdot 10^{-4}\cdot s^{-1}$, $10^{-5}\cdot s^{-1}$.

At the strain rate of $5\cdot 10^{-4}\cdot s^{-1}$ the tests were performed with a hold time of 330 s in tension or in zero – tension conditions (R= 0.1).

During each test the stress response and the hysteresis loop were recorded at intervals.

Table 1 – Chemical composition of AISI 316 stainless steel in wt %.

C	Si	Mn	P	S	Cr
0.053	0.35	1.63	0.020	0.008	16.9
Ni	**Mo**	**Co**	**Cu**	**Sn**	**N**
12.4	2.45	0.023	0.08	0.005	0.082

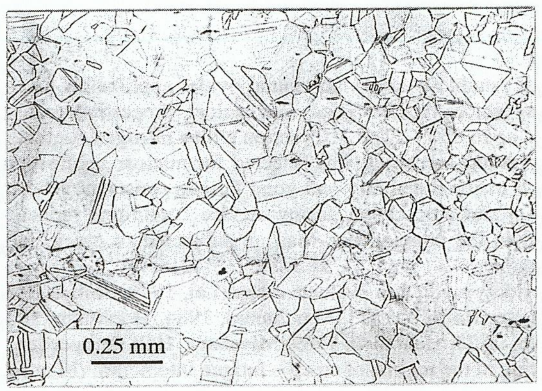

Fig. 1 – Aspect of AISI 316 microsctructure showing austenitic grains.

EXPERIMENTAL RESULTS

The fatigue results are reported in Table 2, where the number of cycles to failure, the total and the plastic strain components, the stress response evaluated at half life and the main experimental parameters are shown. The number of cycles to failure N has been evaluated from the Δσ–n curve of each test. The value corresponds to the point in which a strong variation of Δσ level is observed, due to the presence of unstable macrocrack.

The influence of the strain rate and the hold time is shown in Fig. 2 in which the plastic strain range is plotted versus the number of cycles to failure. The fatigue life is not sensibly reduced, when strain rate changes from $10^{-2}\cdot s^{-1}$ to $10^{-3}\cdot s^{-1}$. Different behaviour is found at lower strain rates and when a hold time is introduced or R ratio is changed. In all these conditions a strong reduction of fatigue life is apparent.

During fatigue testing the alloy exhibits a marked stress hardening that is completed before half life for the experiments run at a total strain over 1%. Figure 3 shows some examples of this behaviour in a stress–strain plot. At high strain levels an initial stress hardening occurs, a plateau is reached and hold, then a stress drop is observed. The stress drop corresponds to the presence of a macroscopic crack that propagates rapidly until final fracture. At low strain levels the strain hardening is present in all the life until macroscopic crack is apparent or final fracture occurs. When the total strain level increases, the strain hardening is increased (200 – 300% at about 1.2% and 30% at about 0.5%).

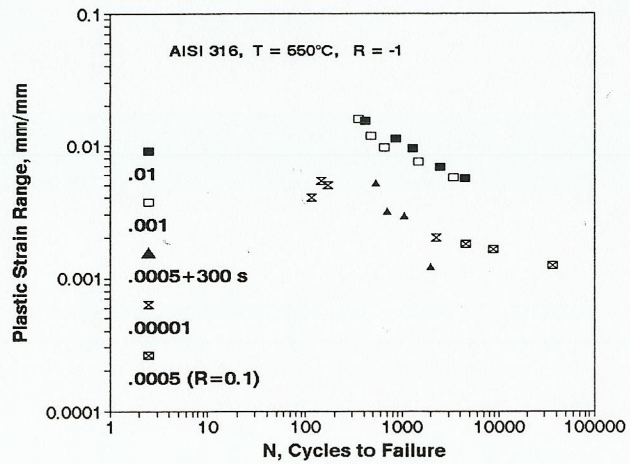

Fig. 2 – Low cycle fatigue results at different experimental conditions.

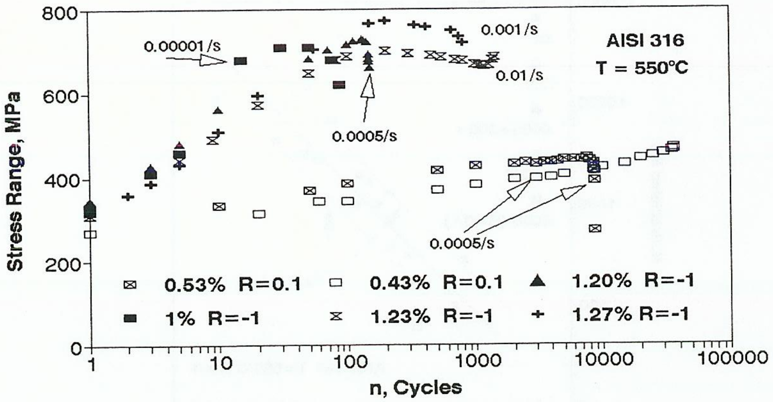

Fig. 3 – Δσ–n curves showing a large strain hardening.

Table 2 – Fatigue results on AISI 316 stainless steel at 550°C.

Strain rate s^{-1}	R	Hold time s	$\Delta\varepsilon_t$ %	$\Delta\varepsilon_p$ %	Δσ MPa	N Cycles
10^{-2}	-1	0	1.95	1.54	850	420
10^{-2}	-1	0	1.46	1.14	750	850
10^{-2}	-1	0	1.23	0.95	700	1300
10^{-2}	-1	0	0.96	0.69	605	2500
10^{-2}	-1	0	0.80	0.56	515	4400
10^{-3}	-1	0	1.96	1.57	900	350
10^{-3}	-1	0	1.51	1.18	820	470
10^{-3}	-1	0	1.26	0.97	760	655
10^{-3}	-1	0	0.99	0.75	670	1450
10^{-3}	-1	0	0.78	0.57	590	3400
5.10^{-4}	-1	300	0.80	0.3125	646	705
5.10^{-4}	-1	300	0.71	0.288	573	1040
5.10^{-4}	-1	300	1.05	0.512	656	530
5.10^{-4}	-1	300	0.40	0.279	466	2000
10^{-5}	-1	0	1.20	0.5375	705	145
10^{-5}	-1	0	1.00	0.50	686	171
10^{-5}	-1	0	0.70	0.20	630	2300
10^{-5}	-1	0	1.00	0.40	719	116
5.10^{-4}	0.1	0	0.43	0.125	435	36700
5.10^{-4}	0.1	0	0.46	0.165	444	8750
5.10^{-4}	0.1	0	0.533	0.179	486	4550

FATIGUE LIFE PREDICTION

One of the methods extensively used for fatigue life prediction is the frequency modified approach in which the Coffin–Mansion (Coffin, 1973) relationship is improved by adding a factor that incorporates the waveform effect. The final expression is as follows:

$$\Delta\varepsilon_p / \varepsilon_f = C \cdot (N \cdot \nu^{K-1})^{-\beta} \quad (1)$$

in which $\Delta\varepsilon_p$ is the plastic strain component evaluated at half life, ε_f the tensile ductility, N the number of cycles to failure, ν the frequency expressed in number of cycles per minute, C, β and K material parameters. The method has been used extensively, with mixed results reported in predicting fatigue lives for several materials (Coffin, 1976, Bernstein, 1982, Batte, 1983).
The values calculated for AISI 316 at 550°C are respectively C = 0.30, β = 0.283 and K = 0.80.
Figure 4 shows the distribution of experimental tests plotted as normalised plastic strain ($\Delta\varepsilon_p/\varepsilon_f$) versus $N \cdot \nu^{K-1}$. ε_f was calculated in correspondence of the first half cycle during each fatigue test and it was observed to be dependent on temperature and strain rate. The ε_f values obtained at different strain rates are reported in Table 3. The tensile ductility generally decreases when the strain rate is reduced. As can be expected, no influence of hold time and R ratio on the tensile ductility value was observed.

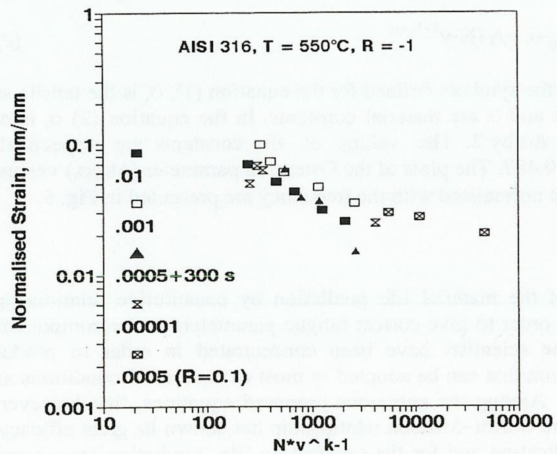

Fig. 4 – Fatigue results plotted according to the equation (1).

Table 3 – Tensile ductility at 550°C for different strain rates.

Strain rate	10^{-2}	10^{-3}	$5 \cdot 10^{-4}$	$5 \cdot 10^{-4}$+HT	$5 \cdot 10^{-5}$
ε_f	0.22	0.16	0.08	0.08	0.06

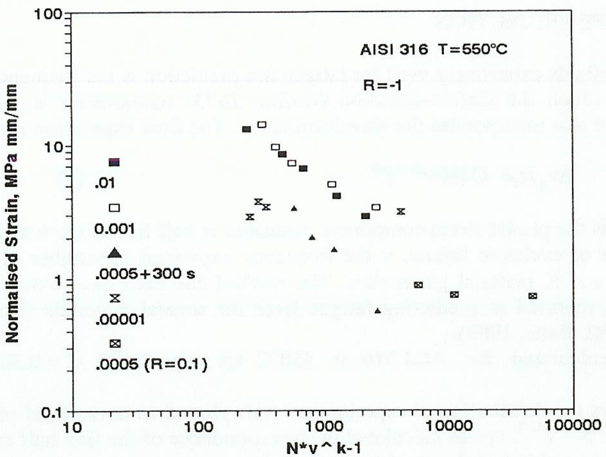

Fig. 5 – Fatigue results plotted according to the equation (2).

Another model frequently used for its simplicity is the Ostergren (1976) relationship modified in order to include time dependent phenomena. The expression is as follows:

$$\Delta\varepsilon_p \cdot \sigma_t = A\,(N \cdot v^{k-1})^{-\alpha} \qquad (2)$$

in which, besides the symbols defined for the equation (1), σ_t is the tensile stress level at half life and A, k and α are material constants. In the equation (2) σ_t is calculated by Table 1 dividing $\Delta\sigma$ by 2. The values of the constants are respectively A = 94.6, k = 0.80, and α= 0.487. The plots of the Ostergren parameter ($\Delta\varepsilon_p \cdot \sigma_t$) versus the number of cycles to failure normalised with the frequency are presented in Fig. 5.

DISCUSSION

The evaluation of the material life prediction by constitutive relationships has been widely studied in order to give correct fatigue parameters to the components designers. The efforts of the scientists have been concentrated in order to produce an ideal constitutive equation that can be adopted in most experimental conditions and for every type of materials. Among the numerous proposed equations, that however can not be used elsewhere, the Coffin–Manson relationship has shown its great efficacy both for its simplicity of application and for the satisfactory life prediction for a large number of materials. If we compare the plots in Fig. 2 with those in Fig. 4 modified according to equation (1), we can deduce that the Coffin–Manson relationship describes the material behaviour with satisfactory accuracy, even when tests are performed at very low strain rates or in presence of hold time. The effect of the equation is to gather the experimental data in one line with a scatterband as small as possible. In this case most of the points lies within a factor 2 scatterband.
The confidence of the models can be observed also in Figs. 6 and 7 in which the predicted life is plotted versus the experimental life. The Ostergren relationship gives an underestimation of the AISI 316 fatigue life for the majority of the experiments. A more accurate prediction is observed using Coffin–Manson relationship.

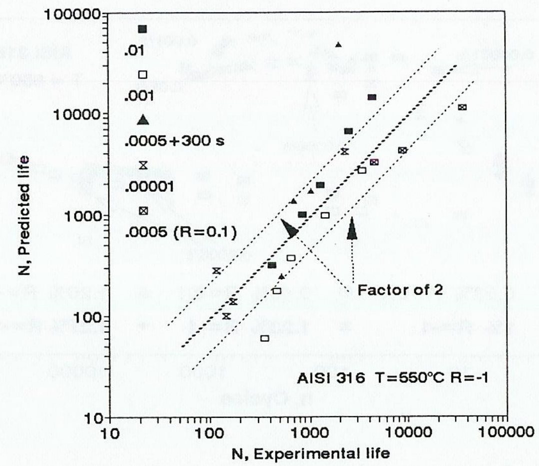

Fig. 6 – Predicted life vs. experimental life for Coffin–Manson relationship.

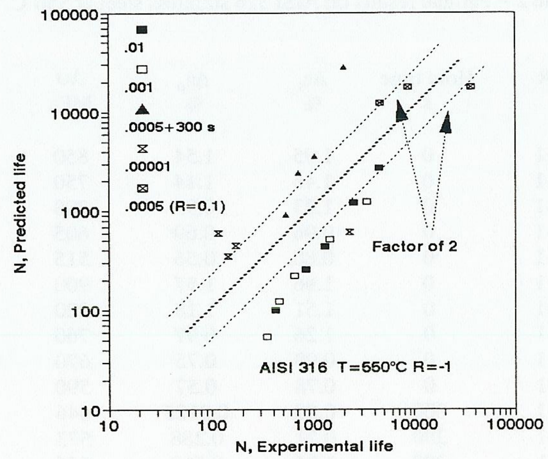

Fig. 7 – Predicted life vs. experimental life for Ostergren relationship.

CONCLUSIONS

The fatigue results at 550°C on AISI 316 stainless steel have shown:

- a reduction of fatigue life, when strain rate decreases or a hold time is superimposed;
- a strain hardening behaviour more marked at the high strain levels and at the low strain rates;
- a satisfactory fatigue life prediction using Coffin–Manson relationship;
- an unacceptable fatigue life prediction when Ostergren approach is utilised.

REFERENCES

Batte, D.A. (1983). *Fatigue at High Temperature,* Applied Science Publ., 365 - 402.

Bernstein, H.L. (1982). Low cycle fatigue and life prediction, *ASTM STP 770,* American Society for Testing and Materials, 105 - 134.

Brinkman, C.R. (1985). High–temperature time – dependent fatigue behaviour of several engineering structural alloys. *Inter. Metals Review,* Vol. 30, **5,** 235 - 258.

Coffin, L.F., Jr. (1973). Fatigue at high temperature, *Fatigue at Elevated Temperatures, ASTM STP 520,* 5 - 34.

Coffin, L.F., Jr. (1976). Proc. of ASME - MPC Symposium on Creep - Fatigue Interaction, MPC - 3, ASME, New York, 349 - 364.

Halford, G.R., M.H. Hirschberg, and S.S. Manson (1973). Temperature effects on the strainrange partitioning approach for creep fatigue analysis, *Fatigue at elevated temperature, ASTM STP 520,* Philadelphia, ASTM, 658 - 667.

Hanninen, H.E. (1979). Influence of metallurgical variables on environment - sensitive cracking of austenitic alloys, *International Metals Reviews,* **3,** 85 - 135.

Korn, C. and G. Pluvinage (1989). Isothermal and thermal mechanical low cycle fatigue of 316L steel, Proc. of ICF7, K. Salama et al. eds., Pergamon Press Pub., Houston, USA, Vol. 2, 1221 - 1228.

Lai, J.K. (1979). A set of master curve for the creep ductility of type 316 steel, *Journal of Nuclear Materials* Vol. 92, 123 - 130.

Manfredi, E., E. Vitale L. Bertin and G. Teano (1982). A review on the creep–fatigue interaction on AISI 304 and 316 stainless steel, Report within the F.R.C.C. group 3 materials. JRC–CEC and University of Pisa Publ., 1 - 43.

Marchionni, M., F. Gabrielli, D. Ranucci and G. Vimercati (1984). High temperature fatigue behaviour of type AISI 316 stainless steel, Proc. of the Conference Amorçage des Fissures sous Solecitations Complexes, Parigi, Societé Francaise de Metallurgie Publ., 263 - 275.

Miyabara, K., D.S. Bae, T. Kimmuce and Y. Shimoide (1995). Change of microstructure and fracture behaviour induced by long term ageing of type 316 stainless steel, Proc. of Materials Ageing and Component Life Extension Symposium, Milano, Italy, EMAS, Publ., 479 - 485.

Ostergren, W.J. (1976). A damage function and associated equations for predicting hold time and frequency effects in elevated temperatures, low cycle fatigue, *Journal of Testing and Evaluation*, Vol. 4, **5,** 327 - 339.

Pineau, A. (1989). Mechanisms of creep - fatigue interaction, *Advance in Fatigue Science and Technology*, Kluwer Academic Publ., 283 - 311.

Piques, R. and A. Pineau (1989). Global and local approach of creep crack initiation and growth on aluminium alloy, Proc. of ICF7, K. Salama et al. eds., Pergamon Press Pub., Houston, USA, Vol. 2, 1707 - 1714.

Shinya, S., T. Nomaka, J. Kyono and T. Takahashi (1986). Evaluation of creep damage of structural metals at elevated temperature. Proc. of the Committee on the High Temperature Strength of Materials, N° 85–4–1 Soc. Mat. Sci., Japan, 7 - 18.

Weiss, B. and R. Stickler (1972). Phase instabilities during high temperature exposure of 316 austenitic stainless steels. *Metall. Trans. A* Vol. 3, **4,** 851 - 866.

Yagi, K., K. Kubo, O. Kanemaru and C. Tanaka (1988). Damage evaluation and life prediction under creep - fatigue loading condition for austenitic stainless steels and low alloy steel in high temperature creep - fatigue, *ASMS,* Japan, Elsevier Applied Science Publ., 115 - 135.